Jittered Random Sampling with a Successive Approximation ADC

Chenchi (Eric) Luo†, Lingchen Zhu⋆
†Texas Instruments, 12500 TI BLVD, Dallas, TX 75243
⋆Georgia Institute of Technology, 75 Fifth Street NW, Atlanta, GA 30308

***Abstract*—This paper proposes a randomly jittered temporal sampling scheme with a successive approximation register (SAR) ADC. The sampling time points are jittered around a uniform sampling clock. A control logic is implemented on a traditional SAR ADC to force it to terminate the sample conversion before reaching the full precision at the jittered time points. As a result, variable word length data samples are produced by the SAR converter. Based on a discrete jittered random sampling theory, this paper analyzes the impact of the random jitters and the resulting randomized quantization noise for a class of sparse or compressible signals. A reconstruction algorithm called Successive Sine Matching Pursuit (SSMP) is proposed to recover spectrally sparse signals when sampled by the proposed SAR ADC at a sub-Nyquist rate.**

***Index Terms*—successive approximation, discrete jittered random sampling**

I. Introduction

The successive approximation ADC [1] is a type of analog-to-digital converter that has resolutions ranging from 8 bits to 18 bits and sampling rates ranging from 50 KHz to 50 MHz. The SAR ADC consists of a few blocks such as one comparator, one digital-to-analog converter (DAC) and one control logic. A special counter called the successive approximation register (SAR) conducts a binary search through all possible quantization levels from the most significant bit (MSB) to the least significant bit (LSB). The resolution of the samples are determined by the number of iterations in the binary search. Denote Δ as the 1-bit quantization time. Ideally, a J-bits resolution can be achieved at a uniform sampling interval of $J\Delta$. [2] was the fist paper that suggested that if we forced the SAR to terminate the binary search at a randomly selected iteration j with variable sampling intervals $j\Delta$, we could still reconstruct a class of sparse or compressible signal even the averaged sampling rate is below the Nyquist rate of the signal. However, [2] fails to analyze the impact of the randomness on the sampled signal spectrum. The proposed reconstruction algorithm in [2] cannot deal with situations when there is a significant spectral leakage which makes the signal not sufficiently sparse in the frequency domain.

This paper aims to analytically associate the exact probability distribution of the sampling jitters with the sampled spectrum and offer a more robust signal reconstruction algorithm in the presence of spectral leakage and randomized quantization noise. The most striking feature of the proposed sampling architecture is that it is compatible with conventional SAR ADC architecture without introducing extra analog mixing circuits as required in [3], [4]. We can easily switch the SAR ADC between a conventional uniform sampling scheme and a jittered random sampling scheme designed specifically to sample a class of spectrally sparse signal with a wider bandwidth coverage. Since the average sampling rate is fixed, the power consumption of the SAR ADC remains unchanged in both schemes.

II. Discrete Time Jittered Random Sampling Theory

The analysis on continuous time random sampling can be traced back to Beutler and Leneman's [5]–[8] publications on the theory of stationary point process and random sampling of random process in the late 1960s. [9] extended the theory to address discrete time additive random sampling. In this section, a theoretical framework for discrete jittered random sampling will be established.

A random impulse process $s(t)$ is defined as

$$s(t) = \sum_{n=-\infty}^{\infty} \delta(t - t_n). \tag{1}$$

A random process $x(t)$ sampled by $s(t)$ can be written as $y(t) = x(t)s(t)$. If t_n is independent from $x(t)$, then

$$\Phi_y(f) = \Phi_x(f) * \Phi_s(f), \tag{2}$$

where $\Phi_y(f)$, $\Phi_x(f)$, $\Phi_s(f)$ are the power spectral densities (PSD) of $y(t)$, $x(t)$ and $s(t)$, respectively. When $t_n = nT$,

$$\Phi_s(f) = \frac{1}{T^2} \sum_{n=-\infty}^{\infty} \delta(f - \frac{n}{T}). \tag{3}$$

Therefore, aliases are periodic replicas of the signal spectrum under uniform sampling. Reference [8] generalized the analytic expression of $\Phi_s(f)$ when i.i.d continuous time jitters u_k is added to the uniform time grid with spacing T.

$$t_k = kT + u_k, \quad u_k \in [-T/2, T/2] \tag{4}$$

$$\begin{aligned}\Phi_s(f) =& \frac{1}{T}\left\{1 - |\psi_{u_k}(2\pi f)|^2\right\} \\ &+ \frac{1}{T^2} \sum_{n=-\infty}^{\infty} |\psi_{u_k}\left(\frac{2\pi n}{T}\right)|^2 \delta(f - \frac{n}{T}).\end{aligned} \tag{5}$$

where $\psi_{u_k}(f)$ is the characteristic function of u_k..

Generally speaking, such kind of jittered random sampling (JRS) is not aliasing free. The n-th aliasing term is scaled by a factor of $|\psi_{u_k}\left(\frac{2\pi n}{T}\right)|^2$. There is also a signal independent noise term $\frac{1}{T}\left\{1 - |\psi_{u_k}(2\pi f)|^2\right\}$ in the power spectrum. However, when u_k is uniformly distributed in $[-\frac{T}{2}, \frac{T}{2}]$, we

978-1-4799-2893-4/14/$31.00 ©2014 IEEE

have

$$\psi_{u_k}(2\pi f) = \frac{\sin(\pi f T)}{\pi f T}, \tag{6}$$

$$\psi_{u_k}\left(\frac{2\pi n}{T}\right) = \delta(n). \tag{7}$$

Equ. (5) becomes

$$\Phi_s(f) = \frac{1}{T}\left\{1 - \left|\frac{\sin(\pi f T)}{\pi f T}\right|^2\right\} + \frac{1}{T^2}\delta(f). \tag{8}$$

Since there is only a single impulse function in $\Phi_s(f)$, uniform JRS is aliasing free from a conventional perspective if the jitters u_k are uniformly distributed in $[-T/2, T/2]$. However, the aliases take another form as a spread spectrum noise term $\frac{1}{T}\left\{1 - \left|\frac{\sin(\pi f T)}{\pi f T}\right|^2\right\}$ in the sampled spectrum, which is referred as the aliasing noise thereafter.

Figure 1 and 2 show the sampled power spectra of an analytic sinusoid with a frequency of 5 Hz with different jitter distributions. The uniform time grid has a spacing $T = 1/3s$ so that the average sampling frequency is below the Nyquist rate of the signal. Aliasing frequencies are present in Fig. 1. Fig. 2 is free from aliasing frequencies. In both cases, there is an non-flat aliasing noise floor in the sampled spectrum.

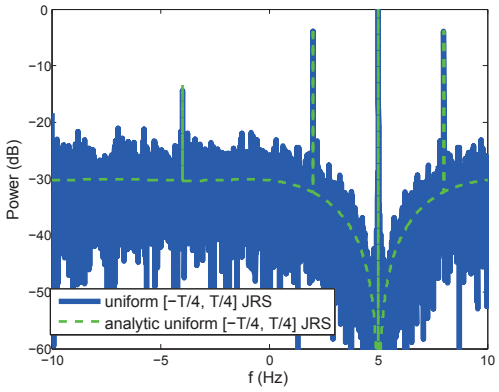

Fig. 1. Power spectra of a sampled analytic signal with a frequency at 5 Hz for uniformly distributed JRS. The uniform time grid has T = 1/3s. The jitters are uniformly distributed in [-T/4, T/4].

In practice, it is difficult to implement continuously distributed jitters. The jitters are usually quantized onto a fixed time grid determined by a high-speed clock. Suppose we further divide the uniform sampling time T into a finer uniform grid with spacing Δ, where $T = J\Delta$ is an integer multiple of Δ, and the jitters u_k are quantized onto the finer uniform time grid, denoted as u_k^q. We can define the probability mass function (PMF) of u_k^q as

$$p[n] = \text{Prob.}\{u_k^q = -T/2 + n\Delta\}, \quad n \in \Omega, \tag{9}$$

where Ω is a subset of $[0, ..., J-1]$.

The time quantization of u_k results in a periodic expansion of its characteristic function $\psi_{u_k}(f)$. Accordingly, $\Phi_s(f)$ also becomes periodic with a periodicity of $\frac{1}{\Delta}$. Therefore, we can ensure that the sampled signal is aliasing free only if $x(t)$ is bandlimited in $[-\frac{1}{2\Delta}, \frac{1}{2\Delta}]$. In other words, the minimum

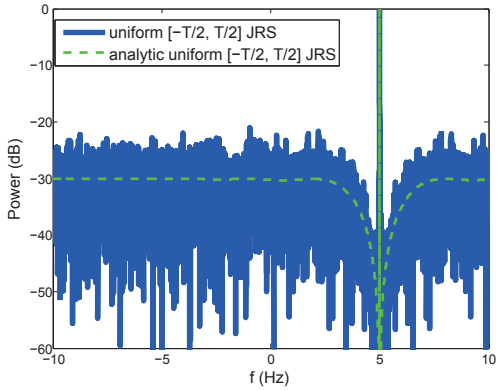

Fig. 2. Power spectra of a sampled analytic signal with a frequency at 5 Hz for uniformly distributed JRS. The uniform time grid has T = 1/3s. The jitters are uniformly distributed in [-T/2, T/2].

spacing Δ rather than the average spacing T of the sampling intervals determines the highest frequency that can be sampled without aliasing. However, sampling at the average sampling frequency is not completely free from the aliasing effect. Aliases in this case are not replicas of the original signal, but behave like an additive noise term convolved with the input signal.

We can define the characteristic function of u_k^q as the discrete time Fourier transform (DTFT) of the PMF of u_k^q:

$$\psi_{u_k^q}(e^{j\omega}) = \sum_{n\in\Omega} p[n]e^{j\omega n}, \tag{10}$$

where the normalized frequency ω is related to the continuous time frequency f by

$$\omega = 2\pi f\Delta. \tag{11}$$

According to (5), the normalized aliasing noise power function for discrete JRS is defined as

$$\Phi_n(e^{j\omega}) = 1 - |\psi_{u_k^q}(e^{j\omega})|^2, \quad \omega \in [0, \pi]. \tag{12}$$

Finally, we assume that the quantized jitter u_k^q is again uniformly distributed on $[-T/2, T/2)$, which means

$$p[n] = \text{Prob.}\{u_k^q = -T/2 + n\Delta\} = 1/J, \quad n = 0, ..., J-1. \tag{13}$$

We will have the following analytic expression for the aliasing noise floor:

$$\Phi_n(e^{j\omega}) = 1 - \frac{1}{J^2}\left(\frac{\sin(\omega J/2)}{\sin(\omega/2)}\right)^2. \tag{14}$$

We can calculate the average power of the aliasing noise floor as

$$\frac{1}{\pi}\int_0^\pi \Phi_n(e^{j\omega})\mathrm{d}\omega = 1 - \frac{1}{J}, \tag{15}$$

which gives a key balancing equation as

$$\underbrace{\frac{1}{\pi}\int_0^\pi \Phi_n(e^{j\omega})\mathrm{d}\omega}_{\text{avg. noise power}} + \underbrace{\frac{\Delta}{T}}_{\text{normalized avg. } f_s} = 1. \tag{16}$$

Equ. (16) represents a fundamental tradeoff between the fine grid granularity Δ and the aliasing noise power. We can choose to make Δ small in order to sample a wider bandlimited signal

$[-\frac{1}{2\Delta}, \frac{1}{2\Delta}]$ at a constant average sampling rate of $\frac{1}{T}$. The downside of the scenario is that we have to endure a higher aliasing noise power. As an extreme case when $\Delta = T$, the aliasing noise term will disappear completely. But the signal is then required to be bandlimited to $[-\frac{1}{2T}, \frac{1}{2T}]$.

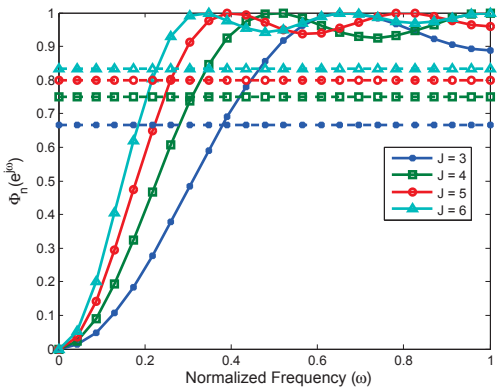

Fig. 3. Aliasing noise power spectra $\Phi_n(f)$ for discrete uniform JRS.

Fig. 3 shows the shape of the aliasing noise function and its average power (horizontal lines) for different choices of the sub-grid division level J. Two important properties of the aliasing noise function can be observed:

$$\Phi_n(e^{j0}) = 0, \tag{17}$$

$$\Phi_n(e^{j\omega}) \leq 1, \tag{18}$$

which means that the aliasing noise floor has no impact at $\omega = 0$, where the original signal frequency resides. And there will not be any overshoots in the aliasing noise floor, which could behave like an impulse function otherwise. These two features makes it easier to extract the original signal from the aliasing noise floor.

III. Amplitude Quantization Error Analysis

Suppose we apply the uniform JRS on a SAR ADC with a fine time grid of spacing Δ and an average sampling spacing $T = J\Delta$, where Δ is the 1-bit conversion time of the SAR ADC and J is the maximum resolution that can be reached. We can implement a control logic to force the SAR ADC to stop the conversion process when a uniform JRS sampling time point is reached. Therefore, the time interval τ between two consecutive samples determines the maximum resolution and the amplitude quantization error that can be reached for the previous sample.

From (13), we can calculate the PMF of the interval τ as

$$p_\tau[n] = \text{Prob.}(\tau = n\Delta) = \begin{cases} \frac{n}{J^2} & n = 1, ..., J \\ \frac{2J-n}{J^2} & n = J+1, ..., 2J-1 \end{cases}. \tag{19}$$

The i.i.d. amplitude quantization error e follows a conditional distribution:

$$e \sim \begin{cases} U[0, \frac{V_{\text{REF}}}{2^n}] & \text{with probability } p_\tau[n], n = 1, ...J-1 \\ U[0, \frac{V_{\text{REF}}}{2^J}] & \text{with probability } \sum_{n=J}^{2J-1} p_\tau[n] = \frac{J+1}{2J} \end{cases}, \tag{20}$$

where U stands for a uniform distribution and V_{REF} is the reference voltage of the ADC. The quantization noise can be modeled as a white noise since e is i.i.d. We can evaluate the power of the noise floor by calculating the expectation and variance of e

$$E[e] = \left[\frac{2^J - J - 1}{2^J J^2} + \frac{J+1}{2^{J+2}J}\right] V_{\text{REF}}. \tag{21}$$

Unlike the uniform sampling case where we only need to encode the signal amplitude, we also need to encode the jitters for the random sampling case, which gives a total of $J + \log_2(J)$ bits/sample.

IV. Signal Reconstruction from The Random Samples

After the data conversion, we can apply DSP techniques to further process the samples. The clocked time quantization in the JRS sampling model makes it possible to calculate the power spectrum using an FFT by replacing missing values with zeros. After we have collected M time quantized samples with

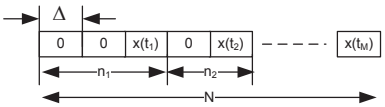

Fig. 4. Interval zero insertion time quantized random samples.

$\{x^q(t_k), n_k\}, k = 1, ..., M$ and $N = \sum_{k=1}^{M} n_k$, we can insert zeros in between each sample according to n_k as shown in Fig. 4. If we denote the zero-inserted signal vector as $\bar{\mathbf{x}}$, then we can calculate the normalized power spectrum by an N-point FFT

$$\mathbf{p} = \frac{1}{M^2}\left|\text{FFT}_N\{\bar{\mathbf{x}}\}\right|^2, \tag{22}$$

Since the minimal time interval is Δ, the frequency grid spacing is $\frac{1}{N\Delta}$ Hz. We refer this zero insertion operation as interval zero insertion (IZI) to distinguish it from the conventional trail zero padding (TZP) operation where zeros are padded at the end of $\bar{\mathbf{x}}$ to reach a higher frequency sampling density. If we are only interested in the detection of certain frequency components from the random samples, calculating the power spectrum is sufficient. In some applications, it is desirable to reconstruct the randomly sampled signal onto a fine uniform time grid so that it can be further processed by classic DSP systems.

However, not all bandlimited signals can be recovered from the random samples because the aliasing noise introduced by the random sampling process could overwhelm the original signal spectrum. Since the aliases are the convolution of the original signal with the aliasing noise function according to the established theory, the aliasing power is proportional to the spectrum occupancy of the original signal. Therefore, only those signals with a sparse spectrum occupancy can be successfully reconstructed. Three factors: aliasing noise, spectral leakage, and amplitude quantization noise make the sampled signal not perfectly sparse in the frequency domain. The aliasing noise floor is introduced by the jittered random

sampling process. The spectral leakage is caused by the finite acquisition time window effect. The amplitude quantization introduces another source of noise that could reshape the total noise floor.

Inspired by the CoSaMP algorithm [10] and the least squares periodogram [11], a new reconstruction algorithm, called successive sine matching pursuit (SSMP), is proposed in this section to deal with the above mentioned factors. The SSMP reconstruction algorithm is summarized in the pseudo code of Algorithm 1. Given M non-uniform samples $\{x^q(t_k), n_k\}$ with a time quantization granularity of Δ, we can calculate the total number of uniform time points N in the acquisition time window. The mainlobe width of each frequency bin is $\frac{2}{N\Delta}$. In the initialization stage, line 3 initializes the reconstructed signal $\mathbf{x}$ to be a zero vector. Line 4 initializes the residual signal $\mathbf{v}$ to be the sampled and amplitude quantized signal $\mathbf{x}_q$. Line 5 evaluates the power in the residual signal $\mathbf{v}$. For each iteration, line 10 performs interval zero insertion (IZI) and trail zero padding (TZP) to $\mathbf{v}$. Line 11 performs an FFT on the resulting vector $\bar{\mathbf{v}}$. Line 12 identifies the frequency f that corresponds to the largest peak in the spectrum. Due to spectral leakage and the amplitude quantization and aliasing noise, the actual signal frequency might deviate slightly from f. Instead of fitting a single sinusoid at f, a cluster of sinusoids with frequencies f_j centered around f are used to fit the residual vector $\mathbf{v}$. The frequency search range Δf is set to be half the width of the mainlobe scaled by a factor $r \in (0, 1)$ as initialized in line 2. The number of sinusoids is denoted as J. Line 14 fits this cluster of sinusoids with frequencies f_j, amplitudes α_j and phases ϕ_j to the residual signal on the sampled time grid t_k according to the least squares criterion. Finally, line 15 subtracts the identified sinusoids from the residual vector. This is a critical step as the removal of the stronger signal frequency components also takes away the stronger sidelobes associated with them. As a result, the weaker frequency components become more salient in the residual spectrum. At the same time, line 16 reconstructs the identified sinusoids on the uniform time grid and adds them to the solution. The algorithm ends as in line 18 when the power in the residual vector can no longer be reduced.

A SAR ADC based random sampling example is shown in Fig. 5, where the input signal $x(t)$ is composed of 10 sinusoids with amplitudes uniformly distributed in [0, 1]V and frequencies randomly distributed in [0, 2.4] MHz. The maximum sampling frequency is $F_s = \frac{1}{\Delta} = 4.8$ MHz. The maximum resolution is set to be $J = 20$ bits so that the average sampling frequency is only $\frac{F_s}{J} = 240$ KHz. The number of random samples is $M = 1024$. SSMP is able to reconstruct the original signal spectrum even a few weak frequency components are buried under the aliasing noise floor. The total bit rate is 5.84 Mb/s with a reconstruction signal to quantization noise ratio (SQNR) of 19.70 dB, which corresponds to an effective number of bit (ENOB) of 3.27 bit/sample. In another word, we need to sample uniformly at a frequency of 4.8 MHz or a bit rate of 15.70 Mb/s to reach the the same level of SQNR as achieved by the jittered random sampling case.

Algorithm 1: SSMP algorithm

Input:
noisy non-uniform samples: $\{x^q(t_k), n_k\}, k = 1, ...M$,
total number of uniform time grid in the time window: $N = \sum_{k=1}^{M} n_k$,
time quantization granularity: Δ,
FFT size: $N_{\text{FFT}} \geq N$,
bandwidth search ratio: $r \in (0, 1)$.
Output:
A reconstructed signal: $x[n] = x(n\Delta), n = 0, ..., N-1$

1 *Initialization:*
2 $\Delta f = \frac{r}{N\Delta}$
3 $\mathbf{x}^0 \in \mathbb{R}^N = \mathbf{0}$
4 $\mathbf{v}^0 \in \mathbb{R}^M = \mathbf{x}_q$
5 $e^0 = \|\mathbf{v}^0\|_2^2$
6 $k = 0$
7 *Iteration:*
8 **repeat**
9 $k = k + 1$
10 $\bar{\mathbf{v}} = \text{TZP}(\text{IZI}(\mathbf{v}^{k-1}))$
11 $\mathbf{p} = \text{FFT}(\bar{\mathbf{v}})$
12 $f = |\mathbf{p}|_{(1)}$
13 $f_j \in [f - \Delta f, f + \Delta f]$
14 $\min_{\alpha_j, \phi_j} \sum_{k=1}^{M} (v(t_k) - \sum_{j=1}^{J} \alpha_j \cos(2\pi f_j t_k + \phi_j))^2$
15 $v^k(t_k) = v^{k-1}(t_k) - \sum_{j=1}^{J} \alpha_j \cos(2\pi f_j t_k + \phi_j)$
16 $x^k[n] = x^{k-1}[n] + \sum_{j=1}^{J} \alpha_j \cos(2\pi f_j n\Delta + \phi_j)$
17 $e^k = \|\mathbf{v}^k\|_2^2$
18 **until** $e^k \geq e^{k-1}$;

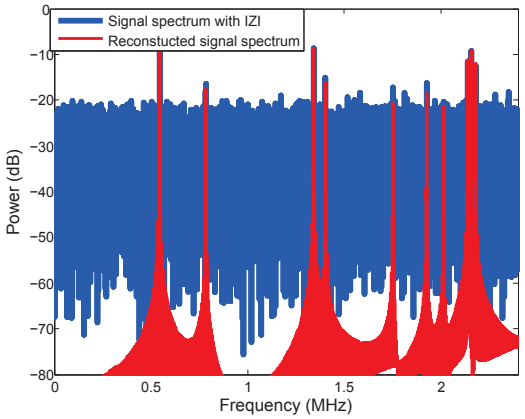

Fig. 5. A comparison between the power spectra by means of direct IZI and reconstruction via SSMP.

REFERENCES

[1] W. Kester, *Analog-Digital Converstion*. Analog Devices, 2004.

[2] C. Luo and J. H. McClellan, "Compressive sampling with a successive approximation adc architecture," in *Acoustics, Speech and Signal Processing (ICASSP), 2011 IEEE International Conference on*, May 2011, pp. 3920 –3923.
[3] J. Tropp, J. Laska, M. Duarte, J. Romberg, and R. Baraniuk, "Beyond nyquist: Efficient sampling of sparse bandlimited signals," *Information Theory, IEEE Transactions on*, vol. 56, no. 1, pp. 520 –544, Jan. 2010.
[4] M. Mishali, A. Elron, and Y. Eldar, "Sub-nyquist processing with the modulated wideband converter," in *Acoustics Speech and Signal Processing (ICASSP), 2010 IEEE International Conference on*, Mar. 2010, pp. 3626 –3629.
[5] F. J. Beutler and O. A. Z. Leneman, "The theory of stationary point processes," *Acta Math.*, vol. 116, pp. 159–197, 1966.
[6] ——, "Random sampling of random process: Stationary point processes," *Information and Control*, vol. 9, pp. 325–344, 1966.
[7] O. A. Z. Leneman, "Random sampling of random process: Impulse processes," *Information and Control*, vol. 9, pp. 347–363, 1966.
[8] F. J. Beutler and O. A. Z. Leneman, "The spectral analysis of impulse processes," *Information and Control*, vol. 12, pp. 236–258, 1968.
[9] C. Luo and J. H. McClellan, "Discrete random sampling theory," in *Acoustics, Speech and Signal Processing (ICASSP), 2013 IEEE International Conference on*, May 2013, pp. 5430–5434.
[10] D. Needell and J. A. Tropp, "CoSaMP: Iterative signal recovery from incomplete and inaccurate samples," *Applied and Computational Harmonic Analysis*, vol. 26, no. 3, pp. 301–321, Apr. 2008.
[11] P. Stoica, J. Li, and H. He, "Spectral analysis of nonuniformly sampled data: A new approach versus the periodogram," *Signal Processing, IEEE Transactions on*, vol. 57, no. 3, pp. 843 – 858, Mar. 2009.